SPANDIDOS PUBLICATIONS

MOLECULAR MEDICINE REPORTS 14: 3301-3306, 2016

Sphingomyelin synthase 2 affects CD14-associated induction of NF-κB by lipopolysaccharides in acute lung injury in mice

SHIDONG HU[1], YI DING[2], JIE GONG[3] and NIANLONG YAN[4]

[1]Department of General Surgery, The General Hospital of Chinese People's Liberation Army, Beijing 100853;
[2]Department of Graduate School, Nanchang University Health Science Center, Nanchang, Jiangxi 330006;
[3]Department of Anesthesiology, The General Hospital of Chinese People's Liberation Army, Beijing 100853;
[4]Department of Biochemistry, College of Basic Medical Science, Nanchang University, Nanchang, Jiangxi 330006, P.R. China

Received June 19, 2015; Accepted July 22, 2016

DOI: 10.3892/mmr.2016.5611

Abstract. Lipopolysaccharide (LPS) is the predominant component of the outer membrane of Gram-negative bacteria, which can cause severe inflammation in the body. The acute lung injury (ALI) induced by LPS can cause extensive damage to the lung tissue, the severe stage of which is termed acute respiratory distress syndrome, when multiple organ dysfunction syndrome may appear. There are no effective clinical treatment measures at present. The involvement of cluster of differentiation (CD)14 assists LPS in causing inflammatory reactions, and CD14 and sphingomyelin (SM), located in lipid rafts areas, are closely associated. SM synthase (SMS) is a key enzyme in the synthesis of SM, however, the effect of SMS on the inflammatory pathway involving nuclear factor (NF)-κB induced by LPS remains to be elucidated. Under the premise of the establishment of an ALI mouse model induced by LPS, the present study established a control group, LPS group and pyrrolidine dithiocarbamate (PDTC; an NF-κB pathway inhibitor) group. Hematoxylin-eosin staining, reverse transcription-quantitative polymerase chain reaction analysis, western blot analysis and thin layer chromatography were used to investigate the mechanism of SMS in ALI. Compared with the control group, the mRNA and protein levels of CD14 were significantly increased ($P<0.001$; n=5 and $P<0.05$, n=5), and the activity of SMS and expression of SMS2 were significantly upregulated ($P<0.001$; n=5 and $P<0.05$, n=5) in the model group. The increases of SMS2 and CD14 in the PDTC group were less marked, compared with those in the model group ($P<0.05$; n=5). These findings suggested that the degree of lung injury was reduced during the acute inflammatory reaction when NF-κB was inhibited, and that the expression of SMS2 may affect the induction of the NF-κB pathway by LPS through CD14.

Correspondence to: Dr Nianlong Yan, Department of Biochemistry, College of Basic Medical Science, Nanchang University, 461 Bayi Road, Donghu, Nanchang, Jiangxi 330006, P.R. China
E-mail: yannianlong@163.com

Abbreviations: LPS, lipopolysaccharide; TLC, thin layer chromatography; ALI, acute lung injury; AS, atherosclerosis; TLR4, toll-like receptor 4; SM, sphingomyelin; HE, hematoxylin-eosin; RT-PCR, reverse transcription-polymerase chain reaction

Key words: sphingomyelin synthase, CD14, lipopolysaccharide, acute lung injury, nuclear factor-κB

Introduction

Lipopolysaccharide (LPS) is the predominant component of the outer membrane of Gram-negative bacteria, a major pathogen causing sepsis. LPS consists of three elements: Lipid A, O side chain antigen and core polysaccharide, of which lipid A is the active center (1). LPS binds to cell surface receptors through lipid A, mediating the occurrence of sepsis. The overexpression of inflammatory mediators by a variety of factors, with the exception of cardiogenic factors, leads to acute lung injury (ALI), causing extensive damage to the lung tissue, the severe stage of which is termed cute respiratory distress syndrome and is followed by multiple organ dysfunction syndrome (2,3). According to the statistics of the US Centers for Disease Control, there are 750,000 cases of serious systemic infections and subsequent disease in the United States each year (4). In China, the morbidity and mortality rates are consistent with those reported abroad (5). Although there has been a focus on basic and clinical investigations of systemic infection in China and abroad, its incidence and mortality rate remain high (6).

The induction of ALI by LPS, which is now considered to be caused by a considerable number of pro-inflammatory and anti-inflammatory agents generated by medullary and/or non-myeloid cells stimulated by nuclear factor (NF)-κB depends on LPS via its associated receptors, cluster of differentiation (CD14) and toll-like receptor 4 (TLR4), and transmembrane signal transduction pathways (7). CD14 is a glycosyl-phosphatidylinositol (GPI)-anchored membrane protein. A previous study determined that GPI-CD14 is predominantly distributed in the sites of membrane lipid rafts (8). As an LPS receptor, CD14 can recognize LPS directly; however, CD14 is not a transmembrane protein, and cannot transfer the stimulation signal between the LPS and

the cytoplasm. It has to transfer signal to the transmembrane protein, TLR4, stimulating the downstream signal substance, activating the nuclear transcription factor, NF-κB, and the expression of a series of inflammatory cytokines, including tumor necrosis factor (TNF)-α, interleukin (IL)-1 and IL-6 (9,10). Studies have suggested that LPS uses its characteristics of inflammation to promote atherosclerosis. For example, following stimulation of mice with LPS, the expression levels of CD14 and TLR4, which are associated with inflammatory signals of monocytes and macrophages, increase. In addition to the high expression levels of CD14 and TLR4, LPS can also significantly increase the expression levels of CD14 and TLR4 in mice with ALI (11,12). Reducing the cholesterol content of lipid raft sites can induce the rearrangement of TNF-α receptor 1 (TNFR1) between lipid and non-lipid raft sites, and can then inhibit inflammation by inhibiting the activation of NF-κB, whereas the inflammatory signaling pathways mediated by TLR4 are suppressed (13-15). The changing content of SM in the lipid raft site can also affect the activation of NF-κB. Meng *et al* (16) used D609 to inhibit the synthesis of SM, which inhibited the activation of NF-κB caused by TNF-α and phorbol myristate acetate (16). Triantafilou *et al* (17) used LPS to stimulate mice, in which the gene for SM had been knocked out, and to also interfere with the synthesis of SM in HEK293 cells. The results demonstrated that, compared with the control group, the activation of NF-κB was significantly reduced, and the recruitment of TNFR1 in the HEK293 cell membrane, caused by the stimulation of TNF-α, was also significantly reduced (17).

SM in cells is synthesized by the catalysis of SM synthase (SMS). SMS is a key enzyme in the final step of a series of enzymatic reactions in SM biosynthesis. It uses ceramide and phosphatidylcholine as substrates to generate SM and diacylglycerol (18). SMS has two isoenzymes: SMS1 and SMS2. SMS1 is located in the intracellular Golgi membranes and SMS2 is located in the cell membrane. They are all closely associated with the structure of the cell membrane, affecting the transmembrane signaling and physiological function of cells (19).

As SMS can catalyze the biosynthesis of SM, the present study investigated the key elements affecting the inflammation signaling pathway (20). Following the stimulation of LPS, the expression of SMS increased in cultured lung cells, however, whether the expression of SMS in experimental mice is affected by LPS requires more detailed investigation. To the best of our knowledge, the association between SMS and the NF-κB pathway induced by LPS remains to be elucidated. In addition, the possible mechanism involving SMS and NF-κB remains to be elucidated. The present study aimed to examine the significant effect of SMS2 during ALI, investigate the possible mechanism involving SMS2 and NF-κB, and provide an important theoretical basis for using SMS2 as a target to treat inflammation-associated diseases, including ALI.

Materials and methods

Animals. A total of 15 clean-level male BALB/c mice, weighing 26±3 g (5-6 weeks old), were supplied by Nanchang University Experimental Animal Center (Nanching, China), and were fed with standard fodder and water and were housed at 25°C. All animal procedures were approved by the Committee on Animal Experimentation of Nanchang University (Nanchang, China), and the procedures complied with the NIH Guide for the Care and Use of Laboratory Animals (21).

Reagents. The reagents used in the present study were as follows: LPS (Sigma-Aldrich; Thermo Fisher Scientific, Inc., Waltham, MA, USA), formalin, β-actin primer, CD14, SMS (Invitrogen; Thermo Fisher Scientific, Inc.), NBD-ceramide, phosphatidylcholine (PC; Santa Cruz Biotechnology, Inc., Dallas, TX, USA), RNA cryoprotectant (ComWin Biotech Co., Ltd., Beijing, China), TRIzol Reagent (ComWin Biotech Co., Ltd.), reverse transcription kit (Takala Biological, Ltd., Dalian, China), 2X Taq Master Mix (Shanghai Welcomes Benro Biotechnology Co., Ltd., Shanghai, China) and CD14 goat anti-mouse antibody (ProteinTech Group, Unc., Chicago, IL, USA).

Preparation of the mouse model of ALI. The 15 BALB/c male mice were randomly divided into three groups: Normal control group, model group and pyrrolidine dithiocarbamate (PDTC; an NF-κB pathway inhibitor) group, with five mice in each group. The model group comprised an LPS copy mouse model of ALI (22). In the PDTC group, PDTC (30 $mg \cdot kg^{-1}$) was injected into the abdominal cavity of the mice prior to model establishment, whereas the mice in the normal control group and model group were injected with equal volumes of DMSO. After 2 h, LPS (10 $mg \cdot kg^{-1}$) was injected into the abdominal cavity of the mice in the PDTC group and the model group, whereas the mice in the normal control group were injected with saline (10 $mg \cdot kg^{-1}$).

Assessment of lung tissue pathology. After 18 h of modeling, all mice were sacrificed by cervical dislocation. The lungs were isolated, washed with saline to remove excess blood, and a 5 μm section of the lung was fixed with 10% formalin for hematoxylin-eosin (HE) staining. Another section of the lung was stored in a -80°C refrigerator to preserve for measurement of SMS activity and western blot analysis. The remaining section of the lung was placed into RNA cryoprotectant and stored at -80°C to detect the mRNA expression levels of CD14 and SMS2.

Reverse transcription-quantitative polymerase chain reaction (RT-qPCR) analysis. Tissues were prepared for RNA extraction by electric homogenization. Total RNA was extracted using TRIzol reagent (ComWin Biotech Co., Ltd.). The primers used were as follows: SMS2, forward 5'-TGTCTGTCCTCGGTTGAAGC-3' and reverse 5'-GGCCTGACCAATGCTCTCTT-3'; CD14, forward 5'-CACAGGACTTGCACTTTCCA-3' and reverse 5'-CTGTTGCAGCTGAGATCGAG-3'; β-actin, forward 5'-ACTCTTCCAGCCTTCCTTCCT-3' and reverse 5'-CAGTGATCTCCTTCTGCATCCT-3'. The reaction mixture for reverse transcription into cDNA was 20 μl, comprising 4 μl dNTP, 4 μl 5X buffer, 2 μl primer mix, 2 μl DTT, 1 μl M-MLVRT reverse transcriptase and 7 μl (2 μg) sample RNA. The sample was mixed at 42°C for 35 min and 85°C for 15 min, and stored at -20°C. For PCR amplification, the sample comprised 0.5 μl upstream primer, 0.5 μl downstream primer, 1 μl, reverse transcribed product, 5 μl 2X Taq

Master Mix and 3 μl ddH_2O. The amplification conditions were as follows: 94˚C for 5 min, 94˚C for 30 sec, 56˚C for 30 sec, 72˚C for 30 sec and 72˚C for 4 min (40 cycles; 28 cycles for β-actin). The amplified products (3 μl) were added to a 2% agarose gel spotting space, and electrophoresis was performed for 20 min under constant 120 V. Quantity One version 4.6.9 software (Bio-Rad Laboratories, Inc., Hercules, CA, USA) was used to analyze the mRNA expression levels of CD14 and SMS2, and calculate the relative expression between these and β-actin.

Thin layer chromatography (TLC) measurement of the activity of SMS. Homogenized buffer was used to extract the total protein of the cells. In brief, the methods of TLC (23) comprised measuring the protein content in each group using a Bradford assay kit (ComWin Biotech Co., Ltd.) and establishing an enzymatic reaction system, according to the following method: 70 μl 10X SMS buffer, 3 μl PC (20 $mg.ml^{-1}$), 4 μl NBD-ceramide (0.5 $mg{\cdot}ml^{-1}$), ddH_2O (X) and crude enzyme extract of SMS (Y). The volume of X+Y (623 μl) was determined, according to the protein content of the crude enzyme extract of SMS in each group adjusted to the specific data of Y, with respect to the volume of the extracted protein, ensuring consistency of the total protein added, with X comprising making the remaining volume. Following mixing in a bath at 37˚C for 2 h, 700 μl of chloroform/methanol (2/1) mixture was added to each tube, vortexed for 1 min, and centrifuged at 8,000 g for 10 min at 25˚C, following which the supernatant was aspirated and equal volumes of the lower organic phase were transferred to a new centrifuge tube containing dry organic solvent with nitrogen. Chloroform (50 μl) was added to dissolve the lipids in each tube, and 50 μl of the chloroform containing dissolved lipid was loaded onto chromatography plates. Chromatography was performed for 10 min in the gel filtration system using a UV irradiated chromatography plate, which can fluoresce enabling the measurement of optical density values. The level of fluorescence and the activity of the enzyme are proportional, therefore, it can indirectly reflect the content of SMS, which reflects the quantity of SMS protein.

Western blot analysis to determinate the expression of CD14. RIPA buffer and PMSF were added to the lung tissue sections and homogenized at 15,000 x g at 4˚C for 5 min, following which PMSF was added prior to incubation on ice for 30 min. The mixture was transferred into centrifuge tubes for centrifugation at 15,000 x g for 15 min at 25˚C. The supernatant of the cell lysates, for separate loading, were conserved at -20˚C. The protein concentrations were determined using a Bradford assay. Equal quantities of the cell lysates (volume x protein concentration 40 μg) were added to equal volumes of 2X electrophoresis sample buffer and boiled in a water bath for 3 min. Electrophoresis of the lysates was performed under constant pressure on an 15% SDS-PAGE gel (separating gel, constant 90 V; separating gel, constant 120 V). Electroblotting was performed according to the manufacturer's protocol, the membranes were washed 2 min after electroblotting and were incubated with 5% skim milk at 4˚C overnight. The membranes were incubated with CD14 primary antibody (goat anti-mouse; cat. no. 17000-1-AP; 1:1,000; ProteinTech Group, Inc., Chicago, IL, USA) and secondary antibody (rabbit anti-goat; cat. no. ab6721; 1:5,000; Abcam, Cambridge, UK) for 1 h at 4˚C, and washed three times following incubation, 10 min each time. Protein was detected using enhanced chemiluminescence fluorescence detection reagent (ComWin Biotech Co., Ltd.) and other enhanced chemiluminescence reagents, and hand-washed with prepared developer and fixer.

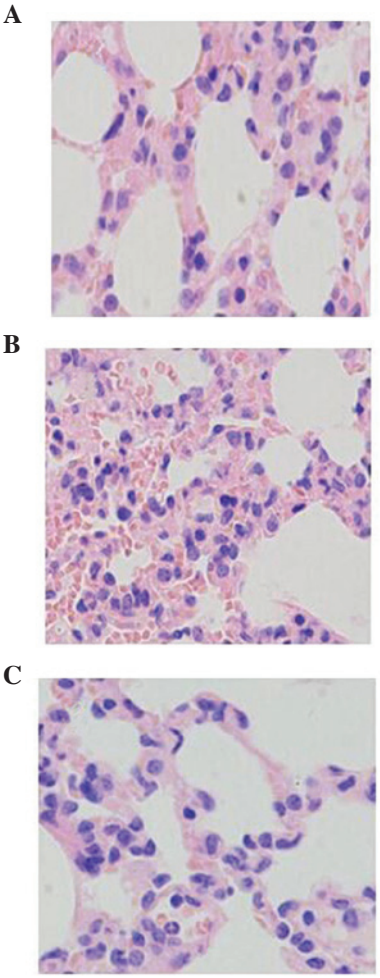

Figure 1. Hematoxylin-eosin staining of mouse lung tissues (magnification, x100). (A) Control group, (B) LPS group, (C) LPS+pyrrolidine dithiocarbamate group. LPS, lipopolysaccharide.

Statistical analysis. Statistical analysis was performed using SPSS 17.0 software (SPSS, Inc., Chicago, IL, USA). All data are expressed as the mean ± standard error of the mean. Differences between groups were assessed using one-way analysis of variance. $P<0.05$ was considered to indicate a statistically significant difference.

Results

Establishment of the mouse model of ALI. Tissue samples of the lungs were examined under light microscopy following HE staining. It was found that the tissues of the normal control group had a clear alveolar structure, thin alveolar wall, and no edema fluid in the alveoli or inflammatory cell infiltration in the interstitial lung (Fig. 1A). Exudate and bleeding were

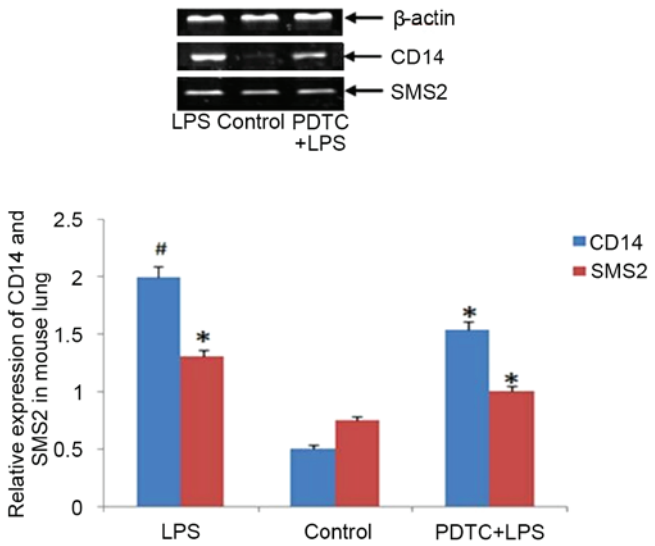

Figure 2. Relative expression levels of CD14 and SMS2 in mouse lung tissues. #P<0.001 and *P<0.05, vs. control (n=5). Data are expressed as the mean ± standard error of the mean. CD14, cluster of differentiation 14; SMS2 sphingomyelin synthase 2; PDTC, pyrrolidine dithiocarbamate; LPS, lipopolysaccharide.

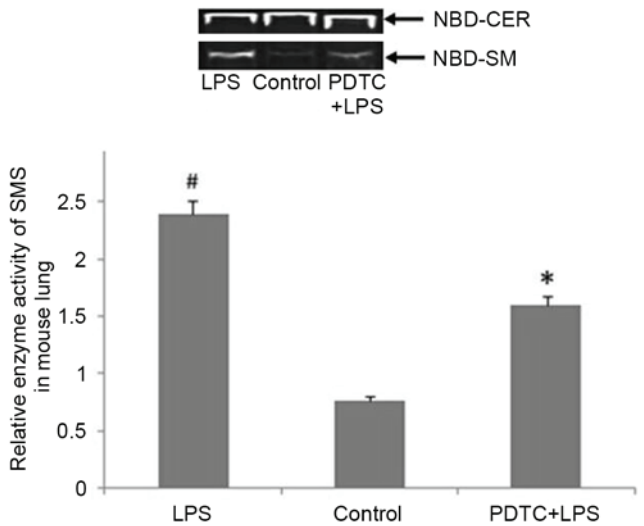

Figure 3. Relative enzyme activity of SMS in mouse lung tissues (#P<0.001 and *P<0.05, vs. control (n=5). Data are expressed as the mean ± standard error of the mean. SM sphingomyelin; SMS, SM synthase; PDTC, pyrrolidine dithiocarbamate; LPS, lipopolysaccharide; CER, ceramide.

observed filling the alveoli in the model group, and the capillaries in the alveolar wall were dilated and congested. There was lymphocyte infiltration of the capillary wall, which was thickened (Fig. 1B). No significant exudate or bleeding of the lung tissues were observed in the PDTC group, with minimal inflammatory cell infiltration and no notable expansion of capillaries in the alveolar wall (Fig. 1C).

mRNA expression levels of SMS2 and CD14. As shown in Fig. 2, compared with the normal control group, the mRNA expression levels of CD14 and SMS2 increased significantly in the model group, being 5.77 and 0.85 times higher, respectively (P<0.001; P<0.05; n=5). The mRNA expression levels of SMS2 and CD14 in the PDTC group were decreased, compared with those in the LPS group, but were higher, compared with those in the normal group, being 3.52 and 0.43 times higher, respectively (P<0.001; P<0.05; n=5). Possibly due to the dose, the inflammation induced by LPS was not completely suppressed by PDTC. The reduction of inflammation resulted in the decline of SMS2 and CD14, which indicated that the change in the levels of CD14 and SMS2 may reduce the reaction to inflammation induced by LPS.

Activity of SMS and protein level of CD14. As shown in Fig. 3, compared with the control group, the activity of SMS of the LPS group was 3.21 times higher, and this difference was significant (P<0.001; n=5). In the PDTC group, the increased activity of SMS was inhibited, however, compared with the control group, the activity of SMS was 2.18 times higher, which was significant (P<0.001; n=5). LPS upregulated the expression of CD14 the protein level, which was 1.34 times higher, compared with that in the control group (P<0.05; n=5). PDTC inhibited the increased expression of CD14, however, the level of CD14 was significantly higher (0.26 times), compared with that in the control group (P<0.05; n=5; Fig. 4).

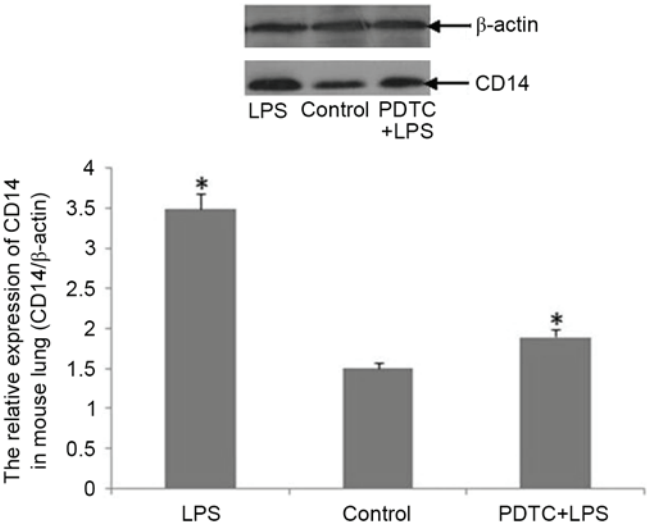

Figure 4. Relative expression of CD14 in mouse lung tissues. *P<0.05, vs. control (n=5). Data are expressed as the mean ± standard error of the mean. CD14, cluster of differentiation 14; PDTC, pyrrolidine dithiocarbamate; LPS, lipopolysaccharide.

Discussion

SM is important in cells and, in addition to being closely associated with the development of AS, it is closely associated with the incidence of cancer. Abalsamo *et al* (24) used D609 to interfere with the synthesis of breast cancer cells, causing a marked decrease in the ability of breast cancer cells to migrate. The analysis of SMS activity and immunohistochemistry of the cancer samples showed that the SMS content in the cancer tissues, were significantly increased, compared with that in paracancer tissues. It has also been suggested that the occurrence of diabetes, obesity and other diseases were linked with SMS. For example, the increase of SM in the cell increases the resistance of the cell to insulin, and

the increase of cellular SM content causes fat accumulation in the liver, leading to fatty liver in mice (25-28). In addition to the occurrence of the above-mentioned diseases, SMS is also involved in the inflammatory response (29). Therefore, SM is closely associated with the occurrence of several diseases, and SMS may be used a target gene in cell and animal experiments.

LPS can induce an acute inflammatory response, which is responsible for ALI. In this process, the signal transduction has been widely recognized, which is mediated by the combination of LPS and CD14, which activate NF-κB. LPS enters the plasma, combining with LPS binding protein (LBP) of the acute phase reaction to form the LPS/LPB complex. This complex can be closely integrated with CD14, forming a complex recognized by the LPS receptor with high affinity (LPS/LBP/CD14) (22). Studies have shown that the CD14/LPS complex can significantly reduce the required concentration of LPS in activating macrophages alone. The sensitivity to LPS in mice with CD14 knockdown has been found to decrease by 1%, compared with the control group (23). However, CD14 is a GPI membrane protein anchored in the cell membrane, which inhibits the transfer of signal transduction independently into the non-intracellular domain (30). As an intracellular receptor associated with LPS transmembrane signal transduction, TLRs can act as LPS signaling receptors when CD14 and LPB are present. The polymerizing activity of TLR4 leads to the activation of myeloid differentiation factor 88, ultimately leading to the activation of NF-κB. The latter induces the synthesis and secretion of inflammatory cytokines, including IL-1β, TNF-α and IL-6, resulting in the synthesis and secretion of increased quantities of inflammatory mediators by effector cells. Thus, a series of pathological reactions are triggered in the body, causing acute inflammatory injury induced by LPS (31-33).

The experimental results in the present study showed that inflammatory exudate and bleeding filled the alveoli of the mice in the model group, which suggested successful model establishment. Compared with the control group, the activity of SMS increased significantly in the model group, as did the mRNA expression levels of CD14 and SMS2, which suggested that the pathological changes of ALI were associated with elevated expression levels of CD14 and SMS2. Pretreating the mice with PDTC significantly reduced the damage from pulmonary edema and hemorrhage induced by LPS. Compared with the model group, the activity of SMS, and the mRNA expression levels of CD14 and SMS2 were decreased, which suggested that PDTC had a protective effect on LPS-induced ALI in mice.

PDTC is an inhibitor of NF-κB. The inflammatory pathological damage in the PDTC group was significantly lower, compared with that in the model group. Following suppression by the NF-κB signaling pathway, the expression levels of SMS2 and CD14 decreased, indicating that SMS2 and CD14 were involved in the NF-κB inflammatory signaling induced by LPS, and that decreasing the levels of SMS2 and CD14 reduced the inflammatory reaction to a certain extent. CD14 is predominantly located in the membrane lipid raft region, which is rich in SM, with SMS2 as the rate-limiting enzyme in SM synthesis. The decreased expression of SMS2 reduced the synthesis of SM, leading to a change in the lipid raft region, and the decreased expression of CD14. Therefore, the present study suggested that SMS2 affected the NF-κB inflammatory signals through CD14.

In conclusion, the present study demonstrated that the degree of lung injury was reduced during the acute inflammatory reaction when NF-κB was inhibited, and that the expression of SMS2 may affect the NF-κB pathways induced by LPS through CD14. These findings provide a theoretical basis in the development of novel drugs for the treatment of ALI.

Acknowledgements

The present study was supported by the National Natural Science Foundation of China (grant no. 81160248) and the National Natural Science Foundation of Jiangxi Province (grant no. 20142BAB205014).

References

1. Zhang L, Wang L, Jiang J, Zheng D, Liu S and Liu C: Lipopolysaccharides upregulate calcium concentration in mouse uterine smooth muscle cells through the T-type calcium channels. Int J Mol Med 35: 784-790, 2015.
2. Vianna RC, Gomes RN, Bozza FA, Amâncio RT, Bozza PT, David CM and Castro-Faria-Neto HC: Antibiotic treatment in a murine model of sepsis: Impact on cytokines and endotoxin release. Shock 21: 115-120, 2004.
3. Chen Y, Zhou X and Rong L: Analysis of mechanical ventilation and lipopolysaccharide-induced acute lung injury using DNA microarray analysis. Mol Med Rep 11: 4239-4245, 2015.
4. Angus DC, Linde-Zwirble WT, Lidicker J, Clermont G, Carcillo J and Pinsky MR: Epidemiology of severe sepsis in the United States: analysis of incidence, outcome, and associated costs of care. Crit Care Med 29: 1303-1310, 2001.
5. Yang Y and Guangxiong Y: Research progress of epidemiology on sepsis J Clin Emer Call 6: 416-420, 2015. (In Chinese)
6. Tadros T, Traber DL, Heggers JP and Herndon DN: Effects of interleukin-1alpha administration on intestinal ischemia and reperfusion injury, mucosal permeability, and bacterial translocation in burn and sepsis. Ann Surg 237: 101-109, 2003.
7. Ulevitch RJ and Tobias PS: Receptor-dependent mechanisms of cell stimulation by bacterial endotoxin. Annu Rev Immunol 13: 437-457, 1995.
8. Lloyd KL and Kubes P: GPI-linked endothelial CD14 contributes to the detection of LPS. Am J Physiol Heart Circ Physiol 291: 473-481, 2006.
9. Gitlin JM and Loftin CD: Cyclooxygenase-2 inhibition increases lipopolysaccharide-induced atherosclerosis in mice. Cardiovasc Res 81: 400-407, 2009.
10. Liu S, Wang H, Qiu C, Zhang J, Zhang T, Zhou W, Lu Z, Rausch-Fan X and Liu Z: Escin inhibits lipopolysaccharide-induced inflammation in human periodontal ligament cells. Mol Med Rep 6: 1150-1154, 2012.
11. Majdalawieh A and Ro HS: LPS-induced suppression of macrophage cholesterol efflux is mediated by adipocyte enhancer-binding protein 1. Int J Biochem Cell Biol 41: 1518-1525, 2009.
12. Wong MC, van Diepen JA, Hu L, Guigas B, de Boer HC, van Puijvelde GH, Kuiper J, van Zonneveld AJ, Shoelson SE, Voshol PJ, *et al*: Hepatocyte-specific IKKβ expression aggravates atherosclerosis development in APOE*3-Leiden mice. Atherosclerosis 220: 362-368, 2012.
13. Miyaso H, Morimoto Y, Ozaki M, Guigas B, de Boer HC, van Puijvelde GH, Kuiper J, van Zonneveld AJ, Shoelson SE and Voshol PJ: Obstructive jaundice increases sensitivity to lipopolysaccharide via TLR4 upregulation: Possible involvement in gut-derived hepatocyte growth factor-protection of hepatocytes. J Gastroenterol Hepatol 20: 1859-1866, 2005.
14. Xie GQ, Jiang JX, Chen YH, Liu DW, Zhu PF and Wang ZG: Induction of acute hepatic injury by endotoxin in mice. Hepatobiliary Pancreat Dis Int 1: 558-564, 2002.
15. Merrill AH Jr and Jones DD: An update of the enzymology and regulation of sphingomyelin metabolism. Biochim Biophys Acta 1044: 1-12, 1990.

16. Meng A, Luberto C, Meier P, Bai A, Yang X, Hannun YA and Zhou D: Sphingomyelin synthase as a potential target for D609-induced apoptosis in U937 human monocytic leukemia cells. Exp Cell Res 292: 385-392, 2004.
17. Triantafilou M, Miyake K, Golenbock DT and Triantafilou K: Mediators of innate immune recognition of bacteria concentrate in lipid rafts and facilitate lipopolysaccharide-induced cell activation. J Cell Sci 115: 2603-2611, 2002.
18. Huitema K, van den Dikkenberg J, Brouwers JF and Holthuis JC: Identification of a family of animal sphingomyelin synthases. EMBO J 23: 33-44, 2004.
19. Yamaoka S, Miyaji M, Kitano T, Umehara H and Okazaki T: Expression cloning of a human cDNA restoring sphingomyelin synthesis and cell growth in sphingomyelin synthase-defective lymphoid cells. J Biol Chem 279: 18688-18693, 2004.
20. Anjum F, Joshi K, Grinkina N, Gowda S, Cutaia M and Wadgaonkar R: Role of sphingomyelin synthesis in pulmonary endothelial cell cytoskeletal activation and endotoxin-induced lung injury. Am J Respir Cell Mol Biol 47: 94-103, 2012.
21. National Research Council Committee for the Update of the Guide for the Care and Use of Laboratory Animals: The National Academies Collection: Reports funded by National Institutes of Health. In: Guide for the Care and Use of Laboratory Animals. National Academies Press (US) National Academy of Sciences, Washington (DC), 2011.
22. Bao Y, Geng Y and Jing H: Effect of hirudin on the levels of acute lung injury rat tumor necrosis factor-α and matrix metalloproteinase-12. Mol Med Rep 5: 873-875, 2012.
23. Le Roy D, Di Padova F, Adachi Y, Glauser MP, Calandra T and Heumann D: Critical role of lipopolysaccharide-binding protein and CD14 in immune responses against gram-negative bacteria. J Immunol 167: 2759-2765, 2001.
24. Abalsamo L, Spadaro F, Bozzuto G, Paris L, Cecchetti S, Lugini L, Iorio E, Molinari A, Ramoni C and Podo F: Inhibition of phosphatidylcholine-specific phospholipase C results in loss of mesenchymal traits in metastatic breast cancer cells. Breast Cancer Res 14: R50, 2012.
25. Adams JM II, Pratipanawatr T, Berria R, Wang E, DeFronzo RA, Sullards MC and Mandarino LJ: Ceramide content is increased in skeletal muscle from obese insulin-resistant humans. Diabetes 53: 25-31, 2004.
26. Górska M, Dobrzyń A, Zendzian-Piotrowska M and Górski J: Effect of streptozotocin-diabetes on the functioning of the sphingomyelin-signalling pathway in skeletal muscles of the rat. Horm Metab Res 36: 14-21, 2004.
27. Straczkowski M, Kowalska I, Nikolajuk A, Dzienis-Straczkowska S, Kinalska I, Baranowski M, Zendzian-Piotrowska M, Brzezinska Z and Gorski J: Relationship between insulin sensitivity and sphingomyelin signaling pathway in human skeletal muscle. Diabetes 53: 1215-1221, 2004.
28. Chen HC, Smith SJ, Ladha Z, Jensen DR, Ferreira LD, Pulawa LK, McGuire JG, Pitas RE, Eckel RH and Farese RV Jr: Increased insulin and leptin sensitivity in mice lacking acyl CoA:diacylglycerol acyltransferase 1. J Clin Invest 109: 1049-1055, 2002.
29. Lou B, Dong J, Li Y, Ding T, Bi T, Li Y, Deng X, Ye D and Jiang XC: Pharmacologic inhibition of sphingomyelin synthase (SMS) activity reduces apolipoprotein-B secretion from hepatocytes and attenuates endotoxin-mediated macrophage inflammation. PLoS One 9: e102641, 2014.
30. Akashi S, Ogata H, Kirikae F, Kirikae T, Kawasaki K, Nishijima M, Shimazu R, Nagai Y, Fukudome K, Kimoto M and Miyake K: Regulatory roles for CD14 and phosphatidylinositol in the signaling via toll-like receptor 4-MD-2. Biochem Biophys Res Commun 268: 172-177, 2000.
31. Dinarello CA: Interleukin-1 and the pathogenesis of the acute-phase response. N Engl J Med 311: 1413-1418, 1984.
32. Heinrich PC, Castell JV and Andus T: Interleukin-6 and the acute phase response. Biochem J 265: 621-636, 1990.
33. Beutler B and Cerami A: Cachectin/tumor necrosis factor: An endogenous mediator of shock and inflammation. Immunol Res 5: 281-293, 1986.